INDUCTIVE COUPLING BETWEEN OVERHEAD POWER LINES AND NEARBY METALLIC PIPELINES. A NEURAL NETWORK APPROACH

Levente **CZUMBIL**, Dan Doru **MICU**, Denisa **ŞTEŢ**, Andrei **CECLAN**
Dep. of Electrotechnics and Measurement, Technical University of Cluj-Napoca, Romania
levente.czumbil@ethm.utcluj.ro

Keywords: electromagnetic compatibility, electromagnetic interference, finite element methods, neural networks, pipelines, transmission lines

Abstract*: The current paper presents an artificial intelligence based technique applied in the investigation of electromagnetic interference problems between high voltage power lines (HVPL) and nearby underground metallic pipelines (MP). An artificial neural network (NN) solution has been implemented by the authors to evaluate the inductive coupling between HVPL and MP for different constructive geometries of an electromagnetic interference problem considering a multi-layer soil structure. Obtained results are compared to solutions provided by a finite element method (FEM) based analysis and considered as reference. The advantage of the proposed method yields in a simplified computation model compared to FEM, and implicitly a lower computational time.*

1. INTRODUCTION

Due to economic policies meat to reduce construction costs and European ecological regulations respectively, various utilities like gas, oil or water transportation pipelines have been forced to share for several kilometers the same distribution corridors as overhead high voltage power lines and/or AC railway systems.

The electromagnetic fields produced by high voltage transmission lines result in AC interference to nearby metallic structures. Therefore, in many situations gas, oil or water transportation metallic pipelines are exposed to the effects of induced AC current and voltages that could be dangerous both on the operating personal and the pipeline structural integrity due to electrochemical corrosion [1-4].

Evaluation of induced currents and voltages in underground metallic pipelines placed in the vicinity of overhead power lines tend to be a complex issue, because many interrelations between them exist. To solve the differential equations which describe the electromagnetic field distribution and the existing coupling mechanism it assumes in most of the cases the use of specific numerical methods, like FEM, which transforms the electromagnetic interference problem into a numerical one [5].

Although FEM yielded solutions are very accurate, regarding to the problem complexity, the computing time of this method increases with the geometry, its mesh and required evaluation parameters. As a result the investigation of HVPL-MP electromagnetic interference problems for different system configurations requires expensive computing time because each new problem geometry involves a new mesh and a new FEM calculations. Therefore, any scaling method of the results from one configuration to another that requires less computing time, may be of interest.

A first attempt in applying artificial intelligence techniques to scale HVPL-MP interference results was made by Satsios et al. [6, 7]. A Fuzzy Logic Block (FLB) was implemented to evaluate the Magnetic Vector Potential (MVP) in case of a phases to ground fault on the HVPL. However, the implemented FLB provide relatively good results, the main disadvantage of this method consists in determination of the optimal parameters, which describes the fuzzy logic rule base. An iterative technique based on conjugate gradient method has been used [6]. Later on a Genetic Algorithm technique had been proposed by Damousis to determine the optimal rule base [8].

Another artificial intelligence approach has been presented by Al-Badi et al. [9, 10] applying a feed-forward Neural Network (NN) to evaluate the induced AC interferences in an underground pipeline in case of a similar phase to ground fault. The main advantage of this NN solution was that it provided directly the value of the induced AC voltages.

Based on the previous experience obtained implementing feed-forward [11] and layer recurrent [12] NN for the evaluation of the MVP in case of phase to ground faults, in the current work the authors have developed a feed forward NN that evaluates directly the HVPL-MP inductive coupling matrix elements. The proposed NN solution enables the evaluation of the induced AC currents and voltages in both HVPL normal operating and phase to ground fault condition, considering a vertically layered soil structure.

2. STUDIED ELECTROMAGNETIC INTERFERENCE PROBLEM

The electromagnetic interference problem between an underground gas transportation metallic pipeline and a nearby high voltage single circuit 220 kV / 50 Hz transmission line is investigated. The underground pipeline and the overhead power line share the same distribution corridor for a distance of 10 km. The induced A.C. currents and voltages in the metallic pipeline are analyzed in both HVPL normal operating and phase to ground fault conditions, when the fault appears far away outside the common right-of-way. For a more realistic problem representation a multilayer earth configuration, with three vertical soil layers is considered, as in *figure 1* can be seen:

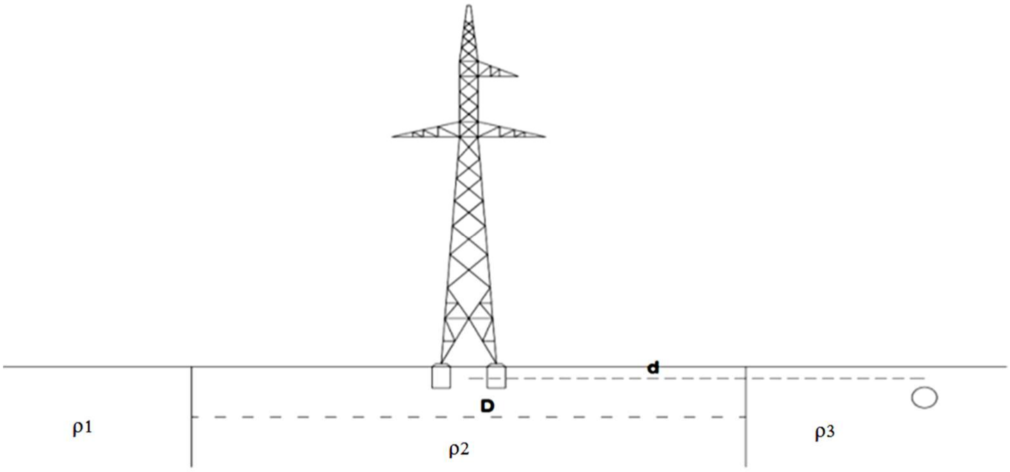

Fig. 1 – Cross section of the investigate electromagnetic interference problem

The underground gas pipeline consists in a steel alloy with a 5.882 MS/m bulk conductivity and a μ_r = 300 relative magnetic permeability. It has 22 cm outer radius a 8 mm thickness and 4.2 mm polyethylene insulation and it is buried at 1.5 m depth. The overhead power line consists in three phase wires and one ground wire placed in delta configuration on IT.Sn102 type metallic transmission line towers. *Table 1* presents the actual position of phase and ground wires on power line towers:

Table 1. Transposing principle

Conductor	Position [m]	Height [m]
Phase Wire A (0°)	2.85	21.4
Phase Wire B (-120°)	-5.3	17.2
Phase Wire C (-240°)	-3.2	17.2
Ground Wire	0	24.7

The electromagnet interference between on overhead transmission line and any nearby metallic structure could be as a results of the following coupling mechanisms [13, 14]:

- Inductive Coupling: Electromotive forces induced by the time varying magnetic field produced by transmission line A.C. currents causes current circulation an voltages between nearby metallic structures and surrounding earth.
- Conductive Coupling: When a ground fault occurs the current flowing through trough transmission line grounding grid produce a potential rise on both the grounding grid and the neighboring soil with regard to remote earth. If the metallic structure is close enough this potential rise could be transferred to it.
- Capacitive Coupling: Affects mostly above ground structures and occurs due to the capacitance between the power line and the nearby metallic structure. Due to earth's screening effect, the capacitive coupling may be neglected in case of underground structures.

Therefore, in our situation, taking into consideration that the phase to ground fault appears far away outside the common right-of-way, only the inductive coupling between the power line and the nearby underground pipeline has to be investigated. For this, first the electromagnetic field distribution around the transmission line has to be analyzed. Considering the cross-section of the common right-of-way the following system of equations describes the linear 2D electromagnetic diffusion problem for the z-direction components A_z of the magnetic vector potential and J_z of the total current density vector is obtained [15]:

$$\begin{cases} \dfrac{1}{\mu_0\mu_r}\cdot\left[\dfrac{\partial^2 A_z}{\partial x^2}+\dfrac{\partial^2 A_z}{\partial y^2}\right]-j\omega\sigma A_z+J_{sz}=0 \\ -j\omega\sigma A_z+J_{sz}=J_z \\ \iint\limits_{S_i} J_z ds = I_i \end{cases} \tag{1}$$

where J_{sz} is the source current density in the z direction and I_i is the imposed current on conductor i of S_i cross section.

Usually equation (1) is solved locally through finite element calculation. Using the values of the magnetic vector potentials, the self and mutual inductances can be calculated using the relations (2) and (3) [16, 17]. Considering a situation where only one of the conductors is energized and a null current is imposed on all the other conductors applying Faraday's Law the self-inductance of energized conductor and the mutual inductance component in all the other conductors due to the energization current can be evaluated based on the magnetic vector potential obtained on the cross-section of each conductor by solving equation (1):

$$L_{i,i}=\frac{\overline{A_{z\,i}}\cdot l}{\bar{I}_i} \tag{2}$$

$$L_{i,j}=\frac{\overline{A_{z\,j}}\cdot l}{\bar{I}_i} \tag{3}$$

where: $L_{i,i}$ and $L_{i,j}$ are conductor i self-inductance and the mutual inductance between conductor i and j respectively, A_{zi} and A_{zj} are the magnetic vector potential on the cross-section of conductor i and j due to energization current I_i and l is the length of the common right-of-way.

Applying a permutation of the energization current on each conductors, one can determine the self and mutual inductance matrix, which describes the inductive coupling between the power line and the nearby gas pipeline [18].

3. NEURAL NETWORK APPROACH

In order to do not rerun the finite element calculation each time a different problem geometry is investigated, the author have developed an artificial neural network that provides the inductive coupling matrix elements for any possible problem geometry. In comparison to previously proposed NN solutions the implemented feed-forward NN allows the evaluation of induced currents and voltages in the underground pipeline for both normal and far away phase to ground HVPL fault operating conditions.

A. The General Structure of an Artificial Neural Network

The concept of an artificial neural network has been inspired by the operation process of the human brain. The major building block of a neural network, the artificial neuron (see *figure* 2), like the biological one is a system with a variable number of inputs u_k, $k=\overline{1,m}$ and only one output.

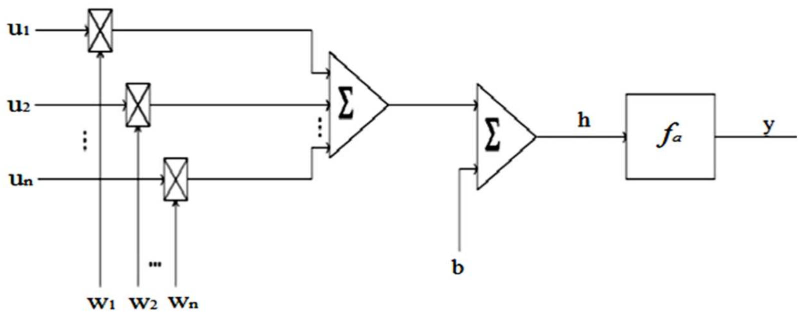

Fig. 2 – Structure of an artificial neuron

The weighted inputs sum is added to a parameter b called bias [18] and provided as argument to a transfer function, which evaluates the output value of the artificial neuron. The transfer function, equation (4), is specific to each neuron and is the equivalent to the nucleus of a biological neuron:

$$y = f_a(h) \text{ where } h = \sum_{k=1}^{m}(u_k \cdot w_k) + b \tag{4}$$

A group of artificial neuron that work in parallel, have the same inputs and the outputs have the same destination form a layer. Multiple interconnected neuron layers form the structure of an artificial neural network. The neurons that provide the output values of the NN form the output layer, whereas all the other neuron layers are called hidden layers. The architecture of neural network is specific to the application for which is implemented. Unusually in electrical engineering applications the classical feed-forward architecture is used (see *figure 3*) [19]:

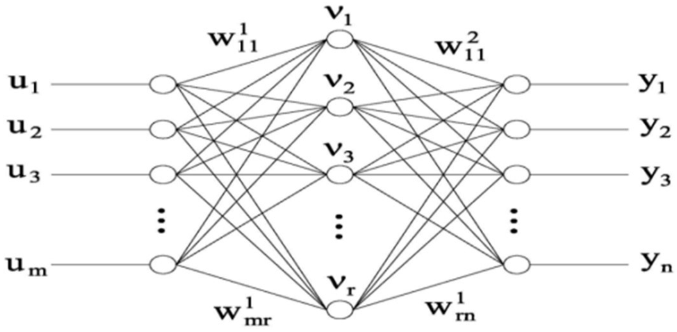

Fig. 3 –Feed-forward neural network with one hidden layer

From the above architecture the equations defining output values of a feed-forward neural network can be developed if the inputs are knowns. The hidden layer neurons output is driven by the following relation:

$$v_j = f_{a1}\left(h_j^1\right) = f_{a1}\left(\sum_k \left(u_k \cdot w_{kj}\right) + b_j^1\right) \tag{5}$$

Therefore, the final outputs of a feed-forward neural network will be given by [19]:

$$y_i = f_{a2}\left(h_i^2\right) = f_{a2}\left(\sum_j \left(w_{kj} \cdot f_{a1}\left(h_j^1\right)\right) + b_j^2\right) \tag{6}$$

In order to provide the desired output values an artificial neural network has to be trained. During the training process the weights and biases of each neuron from the network are continuously adjusted through a back propagation algorithm in accordance to the error between the actual NN output and the desired values. This error is evaluated by a performance function. In most of the cases the mean square error, equation (7), is used as performance function [19]:

$$Err = \frac{1}{n} \cdot \left(\sum_{i=1}^{n} \left(y_i^* - y_i\right)^2\right) \tag{7}$$

B. Proposed Neural Network Implementation

To implement the proposed neural network approach MATLAB's Neural Network toolbox has been used. Based on the previous experience obtained implementing feed-forward [11] and layer recurrent [12] NN for the evaluation of the MVP in case of phase to ground faults, the authors have decided to develop a feed-forward architecture. The input parameters of the proposed NN has been set to:

- d – separation distance between HVPL and MP (which varies between 0 m and 1000 m);
- ρ_1, ρ_2, ρ_3 – resistivity of the left side, middle and right side soil layer respectively (which varies between 10 Ω·m and 5000 Ω·m);
- D – earth middle layer width (which varies between 20 m and 1200 m);

During the pre-processing stage of proposed NN solution all the input parameters are automatically scaled by MATLAB to the [-1,+1] range. The output values are the inductance matrix elements which describe the HVPL-MP inductive couplings. Taking into account that the inductance matrix is a symmetrical one, only the elements above the main diagonal have been considered. Therefore, for the investigated HVPL-MP electromagnetic interference problem (3 phase wires, 1 ground wire and one pipeline) the provided matrix elements will be: $L_{11}, L_{12}, L_{13}, L_{14}, L_{15}, L_{22}, L_{23}, L_{24}, L_{25}, L_{33}, L_{34}, L_{35}, L_{44}, L_{45}, L_{55}$, where L_{ii} representing the self-inductance of conductor i and L_{ij} the mutual inductance between conductor i and j respectively (with for phase wires, i=4 for the ground wire and i=5 for the pipeline).

After analyzing in detail the inductance matrix values obtained through FEM calculation for different problem geometries the authors concluded that in order to increase accuracy and reduce training time to implement three different neural networks: NN1 to evaluate conductors self-inductance $(L_{11}, L_{22}, L_{33}, L44, L55)$, NN2 for the mutual inductances involving the pipeline $(L_{15}, L_{25}, L_{35}, L_{45})$ and NN3 all the other mutual inductance elements.

To train the implemented NN architectures a training data base has been used containing inductive coupling matrix elements obtained through FEM analysis of different

HVPL-MP problem geometries. To obtain a useful training database approximately 4500 different problem geometries have been investigated varying the HVPL-MP separation distance from 0 m to 1000 m, the soil resistivity values from 10 Ω·m to 5000 Ω·m and the middle layer width from 20 m to 1500 m. Table 2 presents some of the problem geometries used to train the implemented neural networks.

Table 2. Training HVPL-MP problem configurations

Case No.	d [m]	D [m]	ρ_1 [Ω*m]	ρ_2 [Ω*m]	ρ_3 [Ω*m]	Case No.	d [m]	D [m]	ρ_1 [Ω*m]	ρ_2 [Ω*m]	ρ_3 [Ω*m]
8	5	60	500	50	500	2134	0	550	50	250	50
104	100	60	150	250	150	2301	20	550	30	250	30
206	20	60	50	500	50	2532	100	550	100	500	100
373	100	60	500	750	500	2751	500	550	30	100	30
481	150	60	500	250	500	2914	5	1050	10	250	10
692	1000	60	750	50	750	3096	20	1050	100	250	100
875	20	120	100	750	100	3274	100	1050	500	1000	500
1064	50	120	750	1000	750	3545	750	1050	30	750	30
1231	500	120	100	30	100	3754	5	1500	50	30	50
1391	0	240	50	10	50	3969	35	1500	10	250	10

1505	0	240	1000	750	1000	4106	750	1500	50	10	50
1891	250	240	500	30	500	4320	1000	1500	250	1000	250
2022	500	240	750	50	750	4442	750	240	50	50	50

In order to identify the optimal solution for each of the proposed neural networks, different feed-forward architectures with one output layer and two hidden layers were implemented (see *figure* 4). The number of neuros in each hidden layer was varied from 5 to 30, the transfer function of the hidden layers were set consecutively to *tansig* (hyperbolic tangent sigmoid function, equation (8)), logsig (logarithmic sigmoid function, equation (9)) and purelin (linear function) whereas the transfer function of the output layer neurons has been set to purelin.

$$f(h)=\frac{1-e^{-2h}}{1+e^{-2h}} \tag{8}$$

$$f(h)=\frac{1}{1+e^{-h}} \tag{8}$$

The performance evaluation function was set to mse (mean square error, equation (7)) and the descendent gradient with momentum weight learning rule was selected to train the neural networks using the Levenberg-Marquardt method.

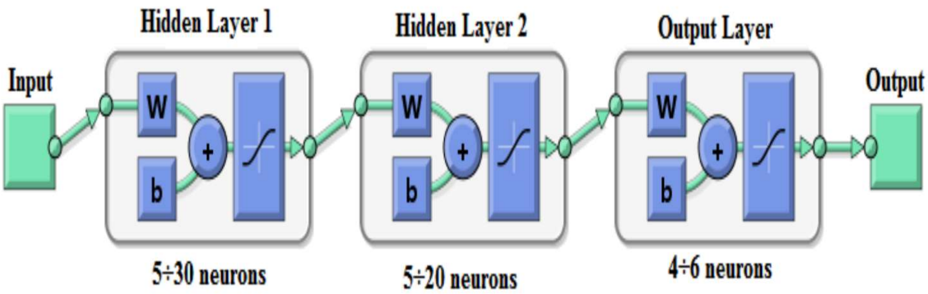

Fig. 4 – Implemented feed-forward network architecture

3. NEURAL NETWORK RESULTS

The training process took between 1 and 10 minutes on a i7-3632QM 2.2GHz Intel Core PC, with a 64 bit operating system and 8 GB RAM memory. Once the implemented neural network architectures were trained, to identify the optimal NN solution, the error between the output values provided by each NN and the finite element results, considered as reference, were evaluated.

Table 3. Testing HVPL-MP problem configuration

Case No.	d [m]	D [m]	ρ_1 [Ω*m]	ρ_2 [Ω*m]	ρ_3 [Ω*m]	Case No.	d [m]	D [m]	ρ_1 [Ω*m]	ρ_2 [Ω*m]	ρ_3 [Ω*m]
1	310	800	900	850	900	15	310	800	900	850	900

3	105	1100	550	550	550	17	170	700	300	350	300
5	250	800	150	150	150	19	240	500	80	750	80
7	340	400	600	150	600	21	420	100	550	20	550
9	170	800	650	750	650	23	105	1200	250	950	250
10	55	1000	900	400	900	25	85	400	140	160	140
11	40	200	600	800	600	28	15	300	140	700	140
13	120	900	750	350	750	30	10	1000	200	750	200

In order to determine the accuracy of the implemented NN architectures in case of new HVPL-MP electromagnetic interference problem configurations, in the NN testing procedure not only the training data base was used, but also a second data set that was not applied during the training process. *Table 3* presents the randomly generated HVPL-MP problem geometries used to test the implemented NN architectures

In case of the neural network used to evaluate the self-inductance of each conductor from the investigate HVPL-MP interference problem, the optimal NN1 architecture is a feed-forward NN with two hidden layers using the *tansig* transfer function: 15 neurons on the first layer and 25 neurons on the second hidden layer. The average evaluation error is 0.043% for the training data base and 0.064% for the testing data set, respectively. The maximum obtained evaluation errors were 0.77% and 0.20% respectively. *Figure 5* presents the error distribution for the training and testing problem geometry data sets:

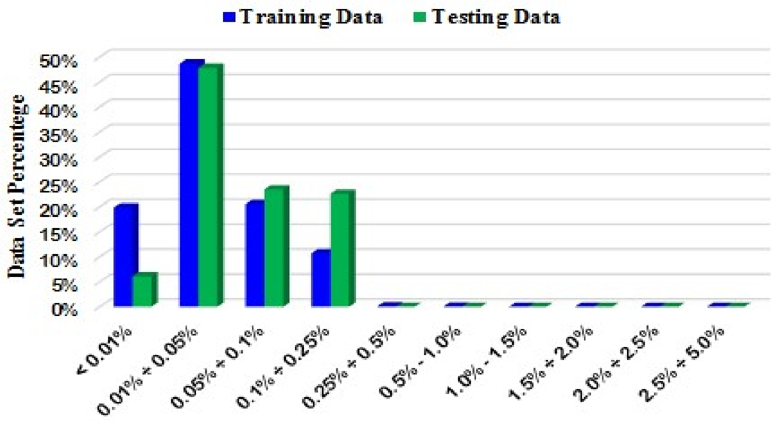

Fig. 5 – Evaluation error distribution for the optimal NN1 architecture

For the neural network implemented to evaluate the mutual inductance values between the underground pipeline and all the other conductors, the optimal NN2 architecture is a feed-forward NN using the *logsig* transfer function and having 30 neurons on the first hidden layer and 25 neurons on the second one. This NN configuration provided an average 0.058% and 0.052% evaluation error for the training data base and the testing data set respectively, whereas the maximum obtained evaluation errors were 2.67% and 0.14% respectively. *Figure 6* presents the error distribution for the training and testing problem geometry data sets:

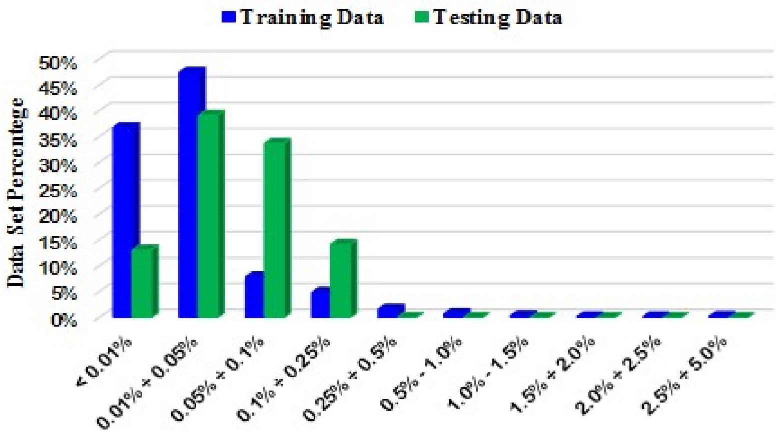

Fig. 6 – Evaluation error distribution for the optimal NN2 architecture

In case of the neural network used to evaluate the mutual inductance values between the HVPL phase and ground wires, the identified NN3 optimal architecture with two hidden layer feed-forward NN with 25, respectively 15 neurons on its hidden layers and using a tansig transfer function. The evaluation error for this optimal NN3 configuration presents and average value of 0.029% and 0.020% for the training and respectively testing data sets, whereas the maximum evaluation error values are 2.56% and 0.069% respectively. Fig. 7 presents the error distribution for the training and testing problem geometry data sets.

Combining the results provided by the above presented three optimal NN configuration the inductive coupling matrix values can be determined for any HVPL-MP problem geometry, with an average 0.1% evaluation error (not exceeding 3% in any case).

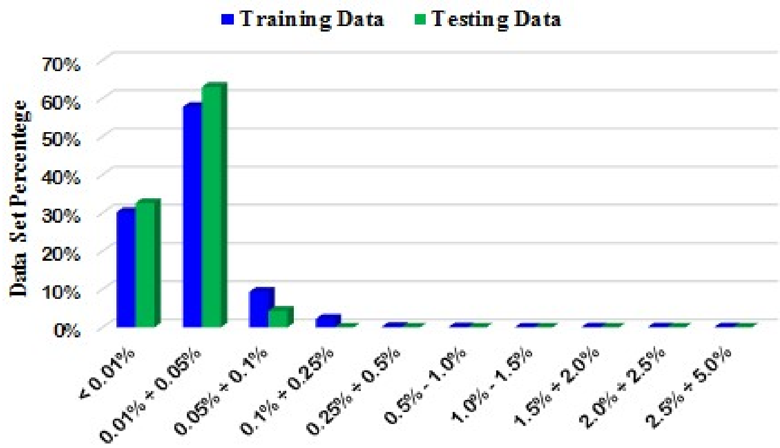

Fig. 7 – Evaluation error distribution for the optimal NN3 architecture

Table 4 presents the obtained self and mutual inductance values describing the inductive coupling between HVPL and the nearby underground pipeline in case of a 30 m separation distance and vertically layers soil structure with ρ_1 = 500 Ω·m, ρ_2 = 30 Ω·m and ρ_3 = 500 Ω·m, considering a 20 m width for the middle layer:

Table 4. Testing HVPL-MP problem configuration

Self and Mutual Inductances [μH/m]					
	PhW A	**PhW B**	**PhW C**	**GrndW**	**Pipe**
PhW A	2.45	1.234	1.110	1.187	0.82
PhW B	1.234	2.45	1.100	1.073	0.84
PhW C	1.110	1.100	2.45	1.073	0.80
GrndW	1.187	1.073	1.073	8.74	0.79
Pipe	0.822	0.842	0.80	0.795	2.28

4. INDUCED CURRENTS AND VOLTAGES

Based on the self and mutual inductance values provided by the proposed neural network solution the equivalent electrical circuit of the investigated HVPL-MP electromagnetic interference problem can be constructed (see *figure 8*). Applying a one side unknown elimination solver based on loop currents method, like the one implemented in the *InterfStud* software application developed by the authors in a previous work [20], the induced A.C. currents and voltages in the metallic pipeline can be evaluated.

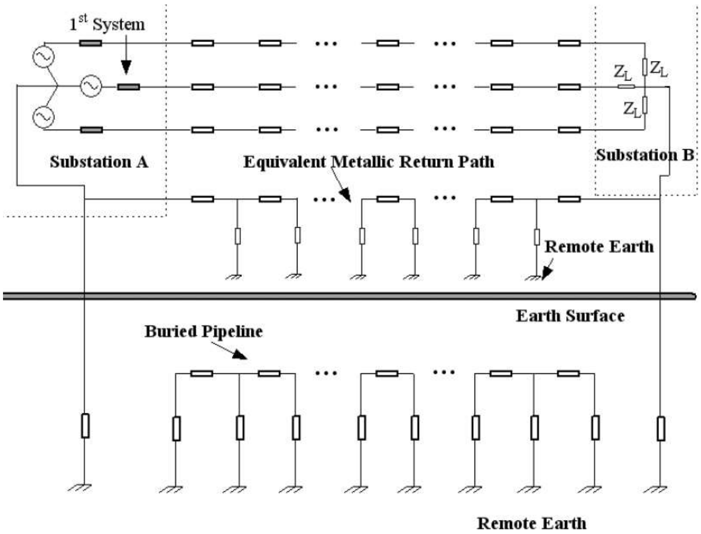

Fig. 8 – HVPL-MP equivalent electrical circuit

A. Steady State HVPL operating conditions

Providing the self and mutual inductance matrix, obtained as output data from the implemented NN solution, to the InterfStud software application the induced current and voltage values have been evaluated considering a steady state HVPL operating condition with a 350 A symmetrical current load on power line phase wires (130 MVA three phase load with a 0.94 power factor). Three different problem geometries have been analyzed:

- ***Geometry 01***. A 30 m HVPL-MP separation distance, considering the following soil structure: $\rho_1 = \rho_3 = 500\ \Omega\cdot$m, $\rho_2 = 30\ \Omega\cdot$m, with a 20 m width middle layer;

- ***Geometry 02.*** A 50 m HVPL-MP separation distance, considering the following soil structure: $\rho_1 = 10\ \Omega\cdot$m, $\rho_2 = 100\ \Omega\cdot$m, $\rho_3 = 500\ \Omega\cdot$m with a 30 m width middle layer;
- ***Geometry 03.*** A 150 m HVPL-MP separation distance, considering the following soil structure: $\rho_1 = \rho_2 = 100\ \Omega\cdot$m, $\rho_3 = 1000\ \Omega\cdot$m, with a 100 m width middle layer;

Figure 9 presents the obtained induced current values along pipeline line length, whereas *figure 10* presents the evaluated induced voltage values. Due the fact that the gas pipeline is electrically insulated at the common right-of-way ends from the rest of the stream gas network the maximum induced voltage level are obtained at right-of-way ends, whereas the induced current reaches its maximum value at right-of-way midsection.

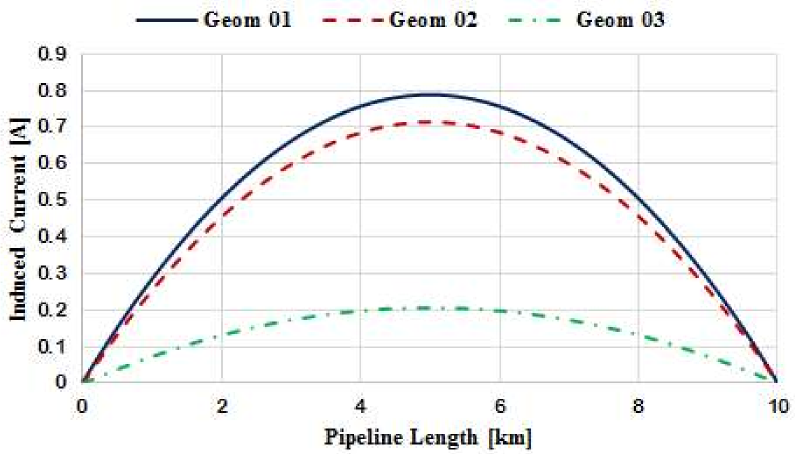

Fig. 9 – Induced current in the underground metallic pipeline for different HVPL-MP problem geometries

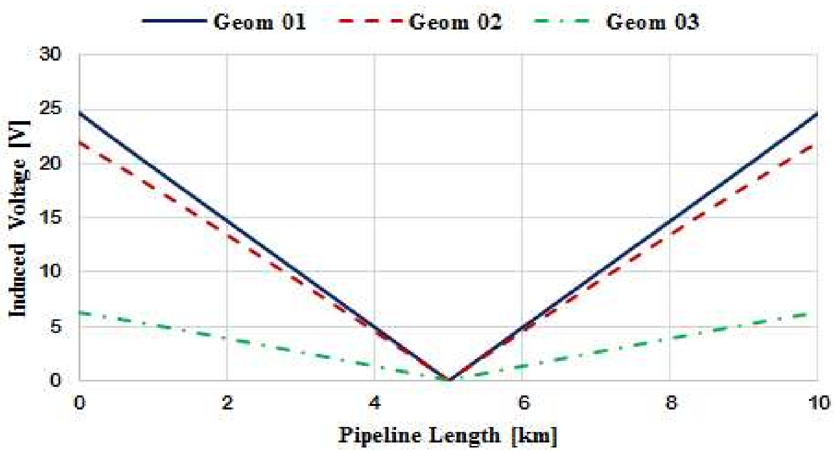

Fig. 10 – Induced voltage in the underground metallic pipeline for different HVPL-MP problem geometries

B. Phase to ground fault HVPL operating conditions

Finally the induced A.C. current and voltages in the underground gas pipeline are evaluated in case of a phase to ground HVPL fault that appears far away outside the common distribution corridor. It is considered that 1500 A current flows through the faulted phase wire (phase A), whereas the same steady state load current flows through the other two healthy phase wires (phase B and C). *Figure 11* presents the obtained induced voltage values along pipeline length for the three investigated problem geometries. It can be observed that the induced voltage values decrease with the separation distance, however an increase is recorded if the soil resistivity in the near proximity of HVPL-MP right-of-way is increased (see *figure 10* and *figure 11*).

5. CONCLUSION

A neural network based artificial intelligence technique has been implemented by the authors to scale from a known set of problem geometries the inductive coupling matrix for any possible geometrical configuration of a HVPL-MP electromagnetic interference. The proposed neural network approach reduces considerably the computation time of the self and mutual inductance values that describe the inductive coupling between the HVPL and the nearby MP.

From *figure 5÷7* it can be observed that the evaluation error produced by the identified optimal NN architecture are usually less than 0.1% in comparison to the finite element results considered as reference. Therefore, the implemented neural network solution to evaluate the self and mutual inductance values is a very effective one, especially if we take into account the fact that the solutions provided by neural networks are obtained almost instantaneously and can be used to evaluate the induced currents and voltages in both HVPL normal and phase to ground fault operating conditions.

ACKNOWLEDGEMENT

This work was supported by the Post-Doctoral Programme POSDRU 159/1.5/S/137516, project co-funded from European Social Fund, through the Human Resources Sectorial Operational Program 2007-2013.

REFERENCES

[1]. CIGRE, *Guide concerning influence of high voltage AC power systems on metallic pipelines*, CIGRE Working Group 36.02, Canada, 1995.

[2]. EN 50443, *Effects of electromagnetic interference on pipelines caused by high voltage A.C. railway systems and/or high voltage A.C. power supply systems*, CENELEC, European Committee for Electrotechnical Standardization, ICS 33.040.20; 33.100.01, January, 2009.

[3]. R. Baboian, *NACE Corrosion Engineer's Reference Book*, NACE International, Huston, USA, 2002.

[4]. R. Zhang, P. R. Vairavanathan, S. B. Lalvani, *Perturbation method analysis of AC-induced corrosion*, Corrosion Science, vol. 50, pp. 1664-1671, 2008.

[5]. D.D. Micu, I. Lingvay, C. Lingvay, L. Darabant, A. Ceclan, *Numerical evaluation of induced voltages in the metallic underground pipelines*, Revue Roumaine des Sciences Techniques Serie Électrotechnique et Énergetique, vol. 54, no. 2, pp. 175-184, 2009.

[6]. K. J. Satsios, D. P. Labridis, P. S. Dokopoulos, *An Artificial Intelligence system for a complex electromagnetic field problem: Part I – Finite element calculations and Fuzzy Logic development*, IEEE Trans. on Magnetics, vol. 35, no. 1, pp. 516-522, 1999.

[7]. K.J. Satsios, D.P. Labridis, P.S. Dokopoulos, *An Artificial Intelligence system for a complex electromagnetic field problem: Part II – Method implementation and performance analysis*, IEEE Trans. on Magnetics, vol. 35, no. 1, pp. 523-527, 1999.

[8]. I.G. Damousis, K.J. Satsios, D.P. Labridis, P.S. Dokopoulos, *Combiend Fuzzy Logic and Genetic Algorithm techniques – Application to an electromagnetic field problem*, Fuzzy Sets and Systems, vol. 129, no. 3, pp. 371-386, 2002.

[9]. A. Al-Badi, K. Ellithy, S. Al-Alawi, *An Artificial Neural Network model for predicting gas pipeline induced voltage caused by power lines under fault conditions*, COMPEL: The International Journal for Computation and Mathematics in Electrical and Electronic Engineering, vol. 24, no. 1, pp. 69-80, 2005.

[10]. A. Al-Badi, K. Ellithy, S. Al-Alawi, *Prediction of voltage on mitigated pipelines paralleling electric transmission lines using an Artificial Neural Network*, The Journal of Corrosion Science and Engineering, vol. 10, Preprint 28, 2007.

[11]. D.D. Micu, L. Czumbil, G.C. Christoforidis, E. Simion, *Neural Networks applied in electromagnetic interference problems*, Revue Roumain des Sciences Techniques, Serie Électrotechnique et Énergetique, vol. 57, no. 2, pp. 162-171, 2012.

[12]. D.D. Micu, L. Czumbil, G.C. Christoforidis, A. Ceclan, *Layer recurrent Neural Network solution for an electromagnetic interference problem*, IEEE Trans. on Magnetics, vol. 47, no. 5, pp. 1410-1413, May, 2011.

[13]. J. Ma, F. P. Dawalibi, *Recent advances in electromagnetic analysis in common corridors*, in Proceedings of the 4th Asia-Pacific Conference on Environmental Electromagnetic (CEEM), pp. 409-418, Dalian, China, 1-4 August, 2006.

[14]. D.D. Micu, A. Ceclan, L. Darabant, D. Stet, *Analytical and numerical development of the* *electromagnetic interference between a high-voltage power line and a metallic underground pipeline*, in Proceedings of the 8th International Symposium on Advanced Electromechanical Motion Systems & Electric Drives Joint Symposium, Lille, France, 1-3 July, 2009.

[15]. G.C. Christoforidis, D.P. Labridis, P.S. Dokopoulos, *Inductive interference calculation on imperfect coated pipelines due to nearby faulted parallel transmission lines*, Electric Power Systems Research, vol. 66, no. 2, pp. 139-148, August, 2003.

[16]. G.C. Christoforidis, D.P. Labridis, *A hybrid method for calculating the inductive interference caused by faulted power lines to nearby buried pipelines*, IEEE Trans. on Power Delivery, vol. 20, no. 2, pp. 1465-1473, April 2005.

[17]. L. Czumbil, D. Stet, D.D. Micu, V. Ţopa. L. Ancas, *Stream gas pipeline in proximity of high voltage power lines. Part II - Induced voltage evaluation*, in Proceedings 47th Internatonal Universities' Conference on Power Energy (UPEC), London, UK, 4-7 September, 2012.

[18]. M. Caudil, C. Butler, *Understanding Neural Networks: Computer Exploration*, vol. 1 and vol. 2, MA: the MIT Press, Cambridge, U.K., 1992.

[19]. S. Razavi, B.A. Tolson, *A new formulation for feedforward Neural Networks*, IEEE Trans. on Neural Networks, vol. 22, no. 10, pp. 1588-1598, 2011.

[20]. L. Czumbil, G.C. Christoforidis, D.D. Micu, D. Stet, A. Ceclan, O. Pop, *A user-friendly software application for induced A.C. interference evaluation*, in Proceedings of the 46th International Universities' Power Engineering Conference (UPEC), Soest, Germany, 5-8 September, 2011.